

# Structural and mechanical properties of TiMnSnAlZrC alloy sintered in different ways

S Gheorghe<sup>1,3</sup>, I Pascu<sup>1</sup>, C Nicolicescu<sup>2</sup> and A Didu<sup>1</sup>

<sup>1</sup> Automotive, Transport and Industrial Engineering Department, Faculty of Mechanics, University of Craiova, Calea Bucuresti Str., no.107, Craiova, 200512, Romania

<sup>2</sup> University of Craiova, Faculty of Mechanics, Department of Engineering and Management of Technological Systems, Drobeta Turnu-Severin (IMST)

<sup>3</sup>stgheo@yahoo.com

**Abstract.** Powder metallurgy is a complex technology that allows obtaining various alloys with special properties which successfully replace alloys achieved by classical technologies. The ability to easily modify classic chemical compositions makes this technology an instrument in the hands of researchers that enables them to always improve the properties of sintered alloys. In addition, the technology itself is very permissive, and new technical solutions can always be found in the technological process of pieces manufacturing. Among the materials very used in the technique, which is very well suited to this technology is titanium. Titanium in combination with other chemical elements greatly improves its operating behavior of obtained material. Therefore, this study proposes a combination of titanium with tin and graphite, recommended for improving wear resistance. The other elements used in the mixture, Al, Zr, Mn help to improve the mechanical properties. The paper intends to present a study on the wear resistance of this Ti alloy, sintered in different ways. SEM and spectrometry analyzes for sintered parts are also presented.

## 1. Introduction

The sintered Titanium alloys are widely used in the technique due to their exceptional physic-chemical, mechanical and technological properties despite the fact that sometimes the cost price is high [1,2]. This is one of the reasons why the manufacturing of alloys with a lower cost price but similar properties has developed. One of the methods used in powder metallurgy is Two-Steps Sintering (TSS) technique which allows for the obtaining of compact components with special properties [3,4].

It is known that all titanium alloys generally have low wear resistance, the improvement of this behavior being always current. Many titanium alloys under light load conditions and relatively low movement can suffer rapid wear which affects the contact surfaces. The surfaces of titanium alloys that are subject to friction have a rapid wear, which leads to their deterioration [5, 6].

Relatively recently, a new technique has emerged that uses the vacuum sintering of titanium hydride powders (TiH<sub>2</sub>) instead of Ti metal powder. During vacuum or inert gas sintering, TiH<sub>2</sub> will dehydrogenize at temperatures below the sintering temperature of Ti alloys, which temperature is generally above 1000°C.

The titanium hydride has good chemical resistance and forms a stable oxide coating on its surface which makes it unreactive in water. Tin has a very good antifriction property, too. It is used both as a

primary element in Sn-Sb type anti-friction alloys and as a secondary element in Cu-Sn or Fe-Sn alloys, for examples, which are recognized as having very good wear resistance.

Ti-Sn alloys have been studied and it has been found that an increase in the concentration of Sn up to 30% leads to the increase of alloy hardness. It has also been found that tin helps titanium in the grinding process, making from these alloys manufactured by mechanical alloying a good alternative [7].

Zr It is very corrosion resistant and is utilized extensively by the chemical industry where corrosive agents are used. Zirconium is similar to titanium, it is compatible with it and a wide range of combinations with other elements such as Al, Sn, C, Nb, are made. Due the properties like ductility and malleability, high melting point, the same atomic structure as titanium, with unlimited solubility, zirconium is an excellent alloying element of titanium, and its alloys are widely used in automotive and space industries [8-13].

Manganese is a hard metal, usually used like an alloying element and in many applications has the same behavior as iron. Manganese is used in steels and cast iron, and its concentration increases when special wear conditions are imposed; manganese is also added to certain types of bronze as well as certain nickel and aluminum alloys. Manganese forms a layer of protective oxide in contact with air, which in the friction conditions improves wear behavior [14,15].

It is also known that carbon in its allotropic graphite form has a very good wear resistance, mainly due to Van der Waals forces. Graphite is the most stable allotrope of carbon and the powder of graphite is an excellent dry lubricant, and its utility in a lot of wear-resistant alloys is so explained [16].

Due to the fact that aluminum, as well the titanium, has a low density but is highly appreciated in various combinations, Ti-Al alloys with high applications in automotive and aerospace technologies are properly studied [17]. The aluminum powder used in these experiments has Si in its component which leads to the increase of refractoriness of the titanium sintered alloy.

## 2. Experiments

The alloy obtained by powder metallurgy technology has the following mass distribution of the components used: 80%wt. TiH<sub>2</sub>, 8%wt. Mn, 6%wt. Alumix321, 3%wt. Sn, 2%wt. Zr, 1%wt. graphite. This combination takes into account the fact that:

- aluminum, oxygen, carbon are the  $\alpha$  stabilizing elements and they increase the allotropic transformation temperature and dissolve in Ti $\alpha$ ;

- manganese and silicon are the  $\beta$  stabilizing elements and they decrease the allotropic transformation temperature, dissolve in Ti  $\beta$  or form eutectoids;

- tin, zirconium are elements with low influence on the transformation temperature.

Titanium hydride, (TiH<sub>2</sub>), produced by Chemetall GmbH, used as precursor material, is the main powder of the mixture and is characterized by a grain-size distribution less than 100  $\mu$ m. The chemical composition of titanium hydride powder, produced by the water-atomizing process, is: titanium min 95%, hydrogen min. 3.8%, nitrogen max.0.3%, Si max.0.15%, Al max.0.15% and Fe, Ni, Cl, Mg, C, Ni each below 0.1%.

Manganese powder, type MN006020, Goodfellow provenience, has maximum particle size: 45micron and Purity 99.5%. The alumix powder 321 is ECKA's provenance and contains Al, Mg, Si, Cu, Fe and lubricant. Zr powder Goodfellow provenance, has a maximum particle size 45micron and purity 99.2. Tin powder, SN006020 Goodfellow provenance has maximum particle size 45micron and purity 99.9%.

The Graphite Powder, is 2N5 American Elements type, with low friction coefficient and 99.5% purity.

The powder used in the mixture analyzed in this paper is presented in the table 1.

**Table 1** The powders used

Elements properties	TiH <sub>2</sub>	Mn	Sn	Alumix 321 [%]					Zr	Graphite	
				Al	Mg	Si	Cu	Fe			lubricant
				balance	0,95	0,49	0,21	0,07	1,50		

Mass [%]	80	8	6	3	2	1
Density[g/cm <sup>3</sup> ]	3,76	7,43	7,29	2,686	6,506	1,8

Planetary Mono Mill PULVERISETTE 6 classic line from Fritsch was used for obtaining a homogenized mixture. The technical conditions were: 250 ml grinding bowl filed with argon atmosphere, 200 rpm for main disk, ball: powders ratio 1.1, balls material stainless steel – 1.3541 ISO/EN/DIN code X47Cr14, B50 and 60 min for mixing time.

A 90Plus particle size analyzer, Brookhaven Instruments Corporation, USA, with 35 mW solid state laser and 660 nm wavelength was used for established the particle size distributions. Grinding in the ball mill only followed a higher homogenization of the mixture and although the working time is relatively low, 60 min, it is found that the resulting particle size is nanometric. The grinding and homogenization operation in the planetary mill with balls results in a granulometric distribution which reveals that the powder obtained has a maximum size of 1,7293  $\mu\text{m}$  while the minimum value is 0,1887  $\mu\text{m}$ . The highest number of particles (28% from the total number) have the dimension equal to 0,2252  $\mu\text{m}$ . The percent of the particles with higher size is lower than 1.5%. The mean hydrodynamic diameter is 0,2911  $\mu\text{m}$ . The percentage of particles, depending on the granulometric distribution, is shown in figure 1.

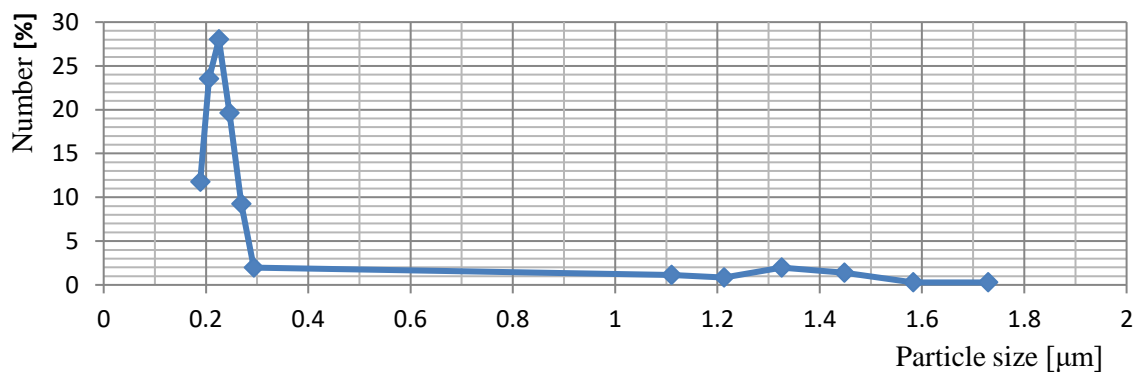


**Figure 1.** Relationship between percentage of particle and granulometric distribution

Selection of sinter mode for titanium alloys is influenced by a number of factors such as the purpose of the alloy, the mechanical and technological properties to be obtained, the alloying elements used, the behavior during heating and, last but not least, the operating costs [18,19,20,22].

Sintering was done in a neutral argon atmosphere and four cycles of work were chosen:

Cycle 1: heating to 1050<sup>o</sup>C and hold for 15 minutes, return to temperature 1000<sup>o</sup>C and maintain for 75 minutes; Cycle 2: heating to 1050<sup>o</sup>C and holding for 90 minutes; Cycle 3: heating to 1050<sup>o</sup>C and hold for 15 minutes, return to temperature 950<sup>o</sup>C and maintain for 75 minutes; Cycle 4: heating to 1050<sup>o</sup>C and hold for 15 minutes, return to temperature 1000<sup>o</sup>C and maintain for 20 minutes, return to temperature 900<sup>o</sup>C and maintain for 55 minutes.

In all four sintering cycles, the maximum temperature was 1050<sup>o</sup>C and the total sintering time was 90 min. The cylindrical samples were analyzed microscopically by an electron microscope based on the 5th generation Phenom desktop SEM platform. Also a spectrometry elemental analysis for all samples was made [16]. These analyses are shown in figures 2-5.

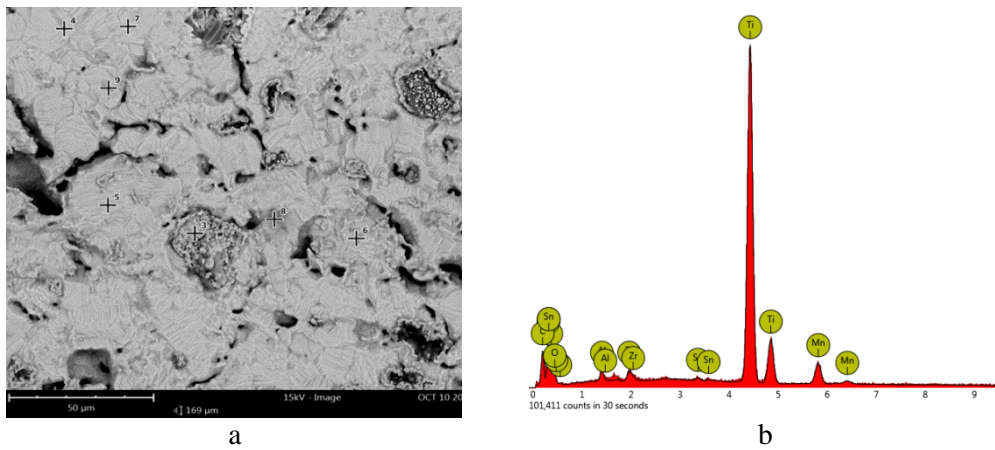


**Figure 2.** a-Scanning electron microscopy (SEM) of sample for Cycle 1;  
b-Spectrometry elemental analysis for SEM cycle 1 spot 6

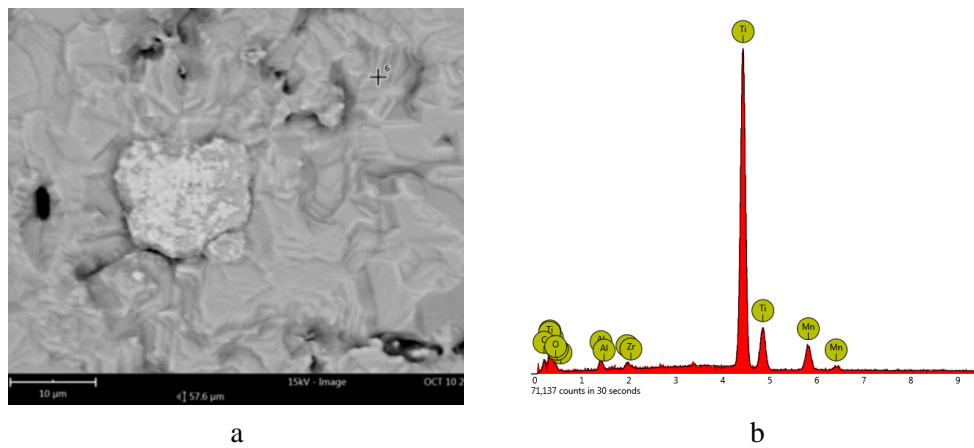


**Figure 3.** a- Scanning electron microscopy (SEM) of sample for Cycle 2;  
b-Spectrometry elemental analysis for SEM cycle 2 spot 6

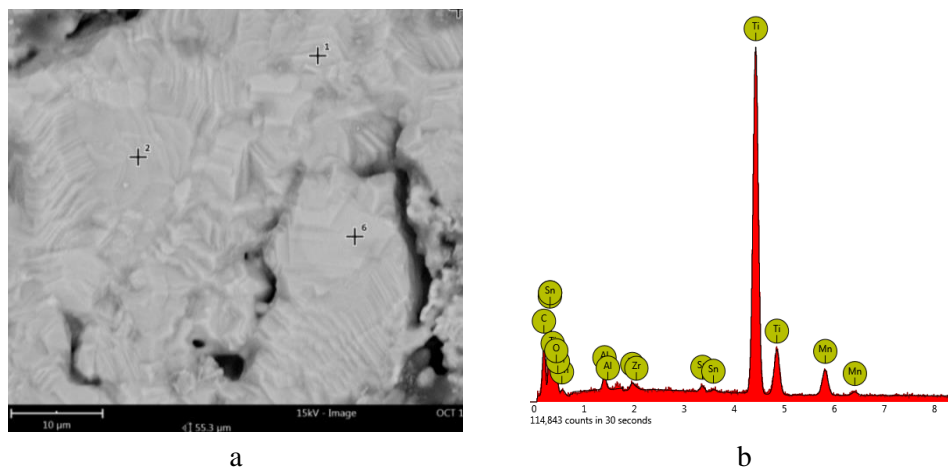


**Figure 4.** a- Scanning electron microscopy (SEM) of sample for Cycle 3;  
b-Spectrometry elemental analysis for SEM cycle 3 spot 6

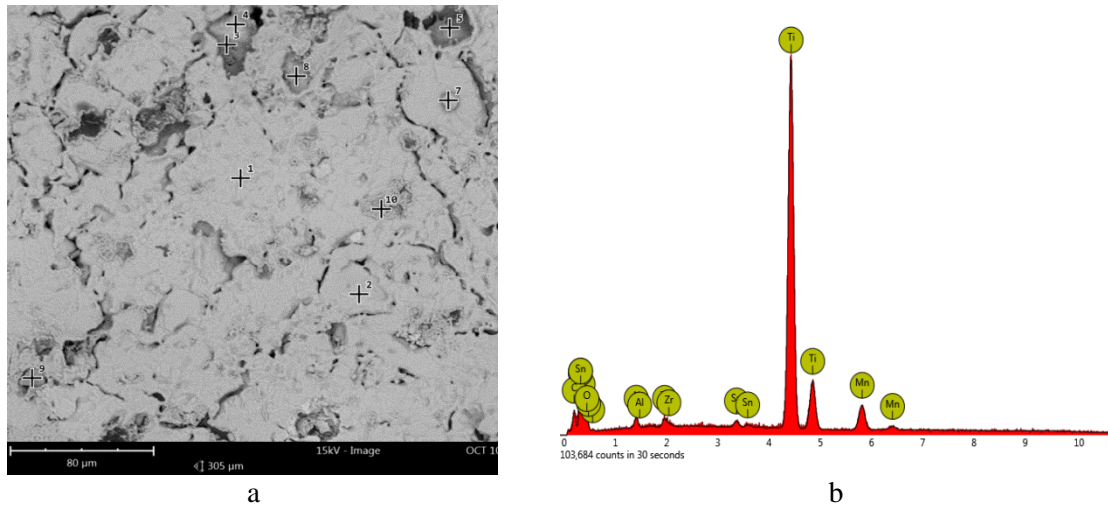


**Figure 5.** a- Scanning electron microscopy (SEM) of sample for Cycle 4; b-Spectrometry elemental analysis for SEM cycle 4 spot 1

Structural analyzes are chemically unattached and highlight a uniform and compact structure of the microstructure of titanium alloy heated in inert gas at 1050 ° C and slowly cooled, shows polyhedral grains. The sintered titanium alloy has  $\alpha + \beta$  structure and this is influenced by the presence of  $\alpha$  stabilizing elements (aluminum, oxygen, carbon),  $\beta$  stabilizers elements (Mn, Si), or low-impact elements ( Sn, Zr). The presence of aluminum in these alloys consists in limiting the range of the solid solution  $\beta$ , increasing the allotropic transformation temperature, increasing the solubility of the isomorphous stabilizing elements  $\beta$ . Spectral analysis shows the presence of all structural elements and also oxygen traces [21].

Titanium and its alloys generally have a low wear resistance, which is why constantly looking for ways to improve this behavior. There are cases where, in addition to changing the chemical composition by adding elements recognized as improving friction behavior, superficial layers are proposed for this purpose.

Wearing attempts have been made in dry friction conditions, as these alloys have elements such as tin or graphite that can work properly in this type of application. For wear testing, sintered cylindrical specimens of titanium alloy 12 mm in diameter were used and the ball was made of steel 100Cr6. A TRB 01-2541CSM Instruments is used to determine the tribo measurement of samples and the test method was ball on disk in the following technical terms, table 2.

**Table 2** Technical conditions for wear test

Static partner	Acquisition	Environment
Substrate: 100Cr6	Radius: 3.00 [mm]	Temperature: 25.00 [°C]
Supplier: CSM	Lin. speed: 6.00 [cm/s]	Atmosphere: Air
Dimension: 6.00 [mm]	Normal load: 2.00 [N]	Humidity: 30.00 [%]
Geometry: Ball	Stop condition: 2000 [lap]	

Surtronic S25 Taylor Hobson Precision profilometer that completes the tribometer product TRB-0254 was used to analyze the wear profile surface. The tribological magnitude curves during the test and the analysis of the profiles of these wear surfaces give us information about the size of the used surface and the magnitude of the resulting depth, are shown in figures 6-9.

For a force of 2 N for 1000 seconds, the experimental results show that the lowest average coefficient of friction, 0.146, was obtained for the fourth cycle. For cycles 1, 2 and 3 the values of the average friction coefficients were propelled by value, namely 0.467, 0.442, 0.431, figures 6-9.a. These values determined for the friction coefficient are considered as average values for this type of alloy. As far as

surface profile analysis is concerned, max depth occurs in Cycle Number 4,  $38.1\mu\text{m}^2$ , while the lowest depth of the used profile,  $19.2\mu\text{m}^2$ , is encountered in Cycle Number 3, figures 6-9.b. The increased presence of oxygen in the structure of alloys manufactured thru cycle number 4 can explain the lower value of friction coefficient and frictional force determined in the contact area.

The wear rate is determined by the amount of material removed, the pressing force and the length of the friction track, following a formula:

$$K = V / F \times S \tag{1}$$

where K is the wear rate in  $[\text{mm}^3/\text{Nm}]$ , F is the force of pressing on the specimens in [N] and S is the length of the friction track, in [m].

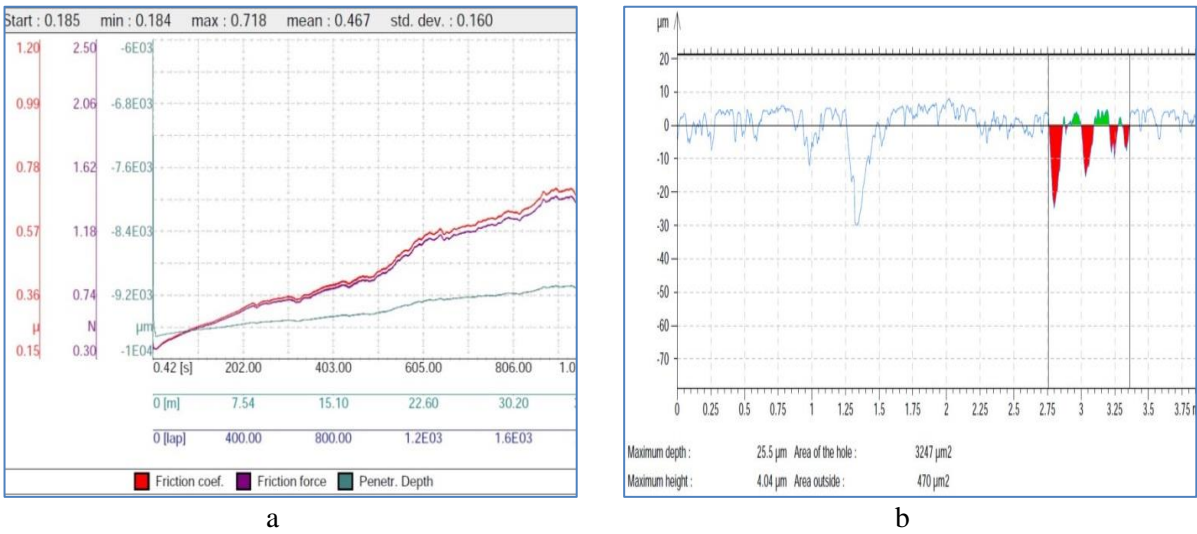


**Figure 6.** Curves of tribological magnitudes during the test (a) and the analysis of the profiles of these wear surfaces for cycle 1 (b)

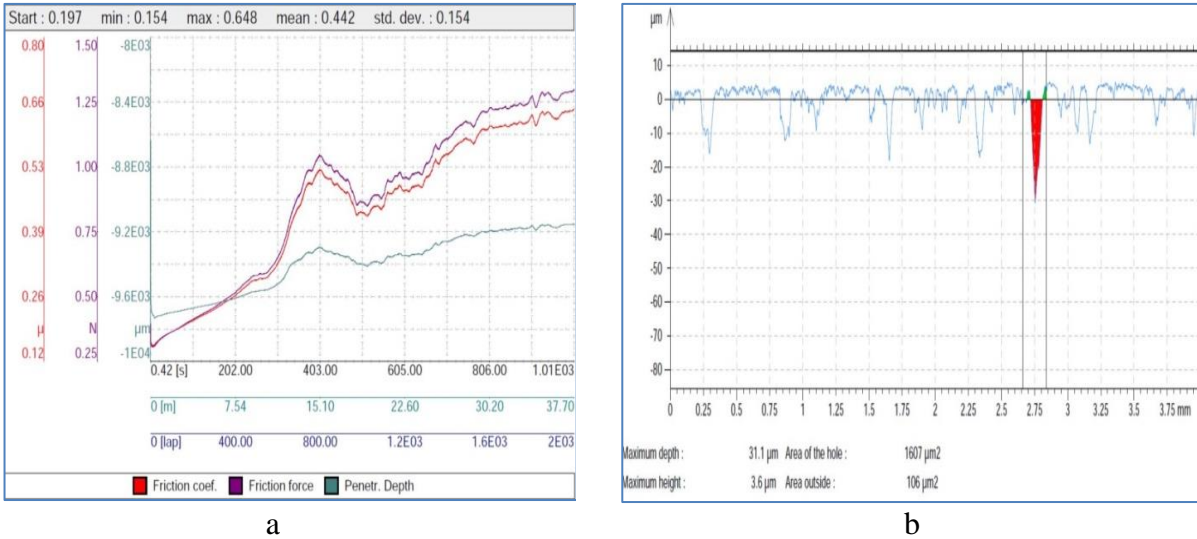
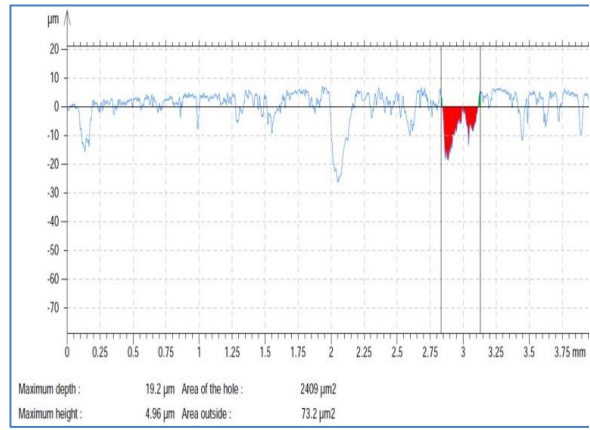


**Figure 7.** Curves of tribological magnitudes during the test (a) and the analysis of the profiles of these wear surfaces for cycle 2 (b)



a

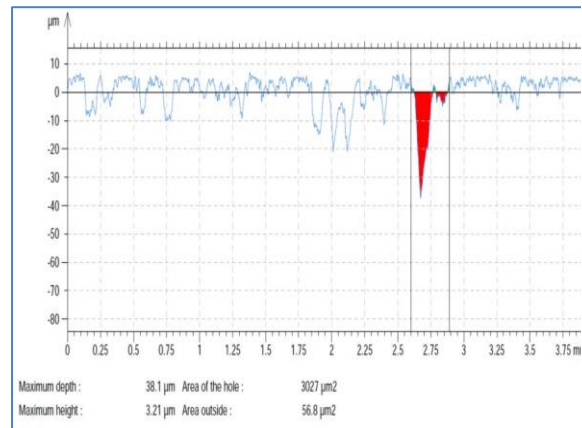


b

**Figure 8.** Curves of tribological magnitudes during the test (a) and the analysis of the profiles of these wear surfaces for cycle 3 (b)



a

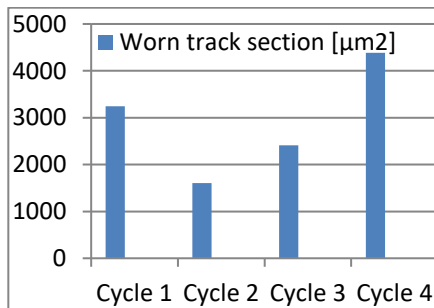


b

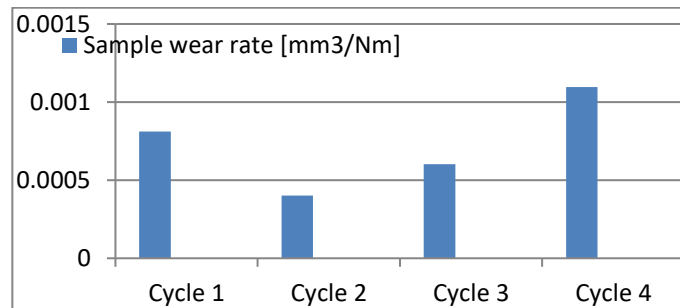
**Figure 9.** Curves of tribological magnitudes during the test (a) and the analysis of the profiles of these wear surfaces for cycle 4 (b)

**Table 3** Wear characteristics

	Cycle 1	Cycle 2	Cycle 3	Cycle 4
Worn track section, [ $\mu\text{m}^2$ ]	3247.0	1607.0	2409.0	4386.0
Sample wear rate, [ $\text{mm}^3/\text{Nm}$ ]	0.0008118	0.0004018	0.0006023	0.001096



a



b

**Figure 10.** a - Worn track section; b - wear rate

The analysis of the experimental results shows that the best wear rates we encounter in the sintering cycle number 2, 0.0004018 mm<sup>3</sup>/Nm, while the lowest value, 0.001096 mm<sup>3</sup>/Nm, is obtained in the sintering cycle number 4, despite the fact that in this case the value of the coefficient of friction has the best value, 0.146, compared to 0.442 in Cycle 2, table 3 and figure 10. These results are also strengthened by the size of the wear sections, which are proportional to wear rates.

## Conclusions

The grinding in planetary ball mills for one hour allows for getting a compact alloy and the particle size drops a lot, reaching nanoscale dimensions.

Multi-step sintering is a variant for titanium-based alloys and this technology may suffer improvements in the future.

The sintering temperature of 1050° C followed by a drop in range of 900° C is the lower limit value that can be used in this type of application.

The wear pattern of the specimens is one that respects the evolution of the phenomenon over time, the graph showing a stabilization of the phenomenon at average values.

The best results of the wear behavior are obtained in the case of sintering at 1050° C with a holding time of 90 minutes, but also the other sintering cycles have comparable values.

The presence of oxygen in the structure of alloys can increase the wear resistance explain the lower value of friction coefficient and frictional force determined in the contact area.

## References

- [1] Boyer R B 2010 *JOM* **62** 35
- [2] Qian M, Schaffer G B, Bettles C J 2010 Sintering of titanium and its alloys *Woodhead Publishing Series in Metals and Surface Engineering*, pp 324-355
- [3] Bartosz W, Waldemar P 2011 *PTCer* **63** 814
- [4] Maca K, Pouch V, Shen Z, 2008 *Integr Ferroelectr* **99** 114
- [5] Goutam D R, Raviraj S, Shrikantha S R, Vinayak N G 2016 *JMR&T* **6** 13
- [6] Budinski KG. 1991 *Wear* **151** 203
- [7] Hsueh-Chuan Hsu, Hsi-Chen Lin, Shih-Ching Wu, Yu-Sheng Hong, Wen-Fu Ho 2010 *J Mater Sci* **45** 1830
- [8] Soyama J, Oehring M, Limberg W, Pyczak F 2015 *Mater Des* **84** 87
- [9] Gabrisch H, Krekeler T, Lorenz U, Rackel M, Stark A 2018 *Mater Sci Forum* **941** 741
- [10] Baker, H.: *Alloy Phase Diagrams* 2006 ASM Handbook, ASM International, Ohio Vol. 3
- [11] Mohammed M T 2017 *Karbala International Journal of Modern Science* **3** 224
- [12] Hsua H C, Wu S C, Sung Y C, Ho W F 2009 *J Alloy Compd* **488** 279
- [13] Benic L, Strkalj A, Glavas Z 2019 *Eng Rev* **39** 115
- [14] Gheorghe S, Teisanu C 2013 *Metalurgia International* **6** 151
- [15] Bolzoni L, Alshammari Y, Yang F 2018 *AMM* **884** 49
- [16] Swee H T, Thampuran R, Goh J, Hong C 1995 Titanium-graphite sintered composite material with improved wear resistance and low coefficient of friction **DE19641023A1**
- [17] Henriques V R et al., 2006 *Mater Sci Forum* **530** 10
- [18] German R M 2014 *Sintering: from Empirical Observations to Scientific Principles* ed. Butterworth-Heinemann (Elsevier USA) pp 471-512
- [19] Yuanshen Qi, Contreras K G, Jung H D, Kim H E, Lapovok R, Estrin Y 2016 *Mater Sci Eng* **59** 754
- [20] Qian Ma, Yang YaF, Shudong D Luo 2015 *Science, Technology and Applications* ed. Butterworth-Heinemann (Amazon USA) pp 201-218
- [21] Pascu C I, Gheorghe St, Nicolicescu C, Tarata D 2018 *Mater Res Proc* **8** 201
- [22] Feng Q, Zhang Y, Dong Z, Zhang P, Wang J, Wang D, Gao Qi, Peng X, Wang F 2018 *Advances in Materials Processing*, (Springer China) **10.1007** 978